

Characterization and Modeling of Diglycidyl Ether of Bisphenol-A Epoxy Cured with Aliphatic Liquid Amines

Nicola T. Guest,^{1,2} David A. Tilbrook,¹ Stephen L. Ogin,² Paul A. Smith²

¹Hexcel Composites, Ickleton Road, Duxford, Cambridge, Cambridgeshire, CB22 4QD, United Kingdom

²Department of Mechanical Engineering Sciences, University of Surrey, Guildford, Surrey GU2 7XH, United Kingdom

Correspondence to: N. T. Guest (E-mail: n.t.guest@gmail.com)

ABSTRACT: The characterization by DMA and compressive stress-strain behavior of an epoxy resin cured with a number of liquid amines is studied in this work along with predictions of the associated properties using Group Interaction Modeling (GIM). A number of different methods are used to assign two of the input parameters for GIM, and the effect on the predictions is investigated. Excellent predictions are made for the glass transition temperature, along with good predictions for the beta transition temperature and modulus for the majority of resins tested. Predictions for the compressive yield stress and strain are less accurate, due to a number of factors, but still show reasonable correlation with the experimental data. © 2013 Wiley Periodicals, Inc. *J. Appl. Polym. Sci.* 130: 3130–3141, 2013

KEYWORDS: mechanical properties; thermosets; structure-property relations; theory and modeling; thermal properties

Received 20 February 2013; accepted 10 May 2013; Published online 13 June 2013

DOI: 10.1002/app.39531

INTRODUCTION

High performance polymer composites are used widely in the aerospace industry, even in safety critical primary structures. At present, development methods for these materials rely on a time consuming and costly process starting with the identification of raw materials and resin formulation stages through to the qualification of the composite parts. With the ever increasing demands being placed on this class of materials, it is desirable to have a deeper understanding of the mechanical and viscoelastic properties of thermosets. Group Interaction Modeling (GIM) has recently been identified as a useful tool to link the chemical structure to the macroscopic material properties of thermoset matrices, and could, therefore, be useful to assist in the development process for polymer composites.

Developed initially by Porter¹ for linear amorphous thermoplastics, GIM has been extended² to predict the properties of highly crosslinked thermosets as a function of temperature and strain rate. It uses a mean field approach to define a constitutive equation of state for an amorphous polymer using multiple molecular input parameters, such as the cohesive energy, number of degrees of freedom, van der Waals volume, chain stiffness, degree of conversion, and activation energy. Most of these parameters can be derived from group contribution tables published by Porter¹ or using molecular modeling techniques.

So far, published work^{2–15} on the validation of GIM has been completed on a number of thermoplastic and thermosetting

polymers, with a significant amount of work being done on multifunctional epoxy resins cured with aromatic amines. Perhaps the most notable of the papers dealing with GIM predictions of thermoplastic polymers, was that by Porter and Gould,³ which extended GIM to include relationships for the post-yield strain softening and hardening effects, validated by experimental data on polycarbonate (PC) and polymethyl methacrylate.

Work done on epoxy resins using the GIM methodology began with Gumen et al.⁷ which focused on predicting the glass transition temperatures of a range of epoxies containing tetraglycidyl 4,4' diaminodiphenylmethane (TGDDM), triglycidyl *p*-aminophenol (TGPAP), 4,4' diaminodiphenylsulfone (4,4'-DDS) and dicyandiamide, which combine to form Hexcel's 924 resin system. In this work, a number of different reaction mechanisms were theorized, with the results highlighting that the accuracy of GIM predictions depends on good knowledge of the reaction chemistry. Liu et al.⁸ used GIM to predict the glass transition temperature of nine stoichiometric resins, namely TGDDM, TGPAP, and DGEBA (diglycidyl ether of bisphenol-A) cured with 4,4'-DDS, diethyltoluenediamine, and dimethylthiitoluenediamine, along with four nonstoichiometric mixes of TGDDM and 4,4'-DDS. Here, the moieties of each epoxy/amine were calculated using a Monte Carlo simulation before the percentage of each was used in the GIM predictions, with the results showing that a difference in structure has a significant impact on the T_g predictions.

A significant amount of work has been carried out by Foreman et al.^{2,9–13} on the validation of GIM for epoxy resins focusing on

TGDDM, TGPAP, and 4,4'-DDS. Foreman et al.² extends previous validation to include a wider range of properties including the stress-strain response, glass and beta transitions, density and linear thermal expansion coefficient of TGDDM/4,4'-DDS, giving predictions that are in excellent agreement with experimental data. This work was extended,¹² to predict a number of properties of TGDDM/4,4'-DDS and TGPAP/4,4'-DDS as a function of strain rate and temperature, which show good agreement with experimental data. Further work by Foreman et al.¹³ included predictions for the same resins as well as a 50 : 50 blend of both TGDDM and TGPAP cured with 4,4'-DDS. In this work, the effect on yield stress and modulus of changing from 4,4'-DDS to 3,3'-DDS, along with changing the central functional group in a Bisphenol epoxy, is also investigated.

Work by Ersoy et al.^{14,15} further extends the work by Foreman et al.⁹⁻¹¹ by using GIM predictions for the stress-strain response of Hexcel 8552 resin in FEA models, to predict the modulus and other properties of AS4/8552 composite, with good agreement against literature values.

This study seeks to extend the validation of GIM to a different range of network structures, dealing with DGEBA, in the form of Epikote 828, cured with a number of aliphatic and cycloaliphatic liquid amines in their ideal stoichiometric ratio (i.e., one mole of active hydrogen to one mole epoxy ring). These liquid amines are Jeffamines D-230, D-400, T-403, and EDR-176, along with IPDA (isophorone diamine), PACM (bis *p*-aminocyclohexyl methane), and a 50 : 50 mix by weight of IPDA and TTD (4,7,10-trioxatridecane-1,13-diamine). In this work, experimental data determined from dynamic mechanical analysis (DMA) and compressive stress-strain tests are compared with the results from GIM predictions. An attempt is made to see if accurate predictions using GIM for this group of resins can be made, based on simple assumptions of network structure, without the need for more complex modeling, such as that employed by Liu et al.⁸ A significant aspect of the work is the characterization and modeling of the subambient beta transition seen on the tan-delta DMA curves, and the assignment of an activation energy, which GIM uses to predict the peak value of this beta transition.

GROUP INTERACTION MODELING

Background Theory

This section provides details of the GIM method used, which matches the method used in work by Foreman et al.² and includes the extension by Porter and Gould,³ to account for post-yield stress relaxation. GIM uses the intermolecular energy of interaction between groups of atoms in adjacent polymer chains as a basis for its predictions. It combines the Lennard-Jones potential function for nonbonded chain interaction and a thermodynamic balance of the different energy contributions. Together, this forms an equation of state (or thermodynamic potential function) for the total energy E_{total} in the system.

$$E_{\text{total}} = \phi_0 \left[\left(\frac{V_0}{V} \right)^6 - 2 \left(\frac{V_0}{V} \right)^3 \right] = 0.89 E_{\text{coh}} - H_T \quad (1)$$

The total energy is comprised of cohesive, configurational, and thermal energy contributions. The cohesive energy, E_{coh} relates to

the depth of the potential energy well, ϕ_0 in the Lennard-Jones function at r_0 with volume V being proportional to r^2 , the separation distance squared. The configurational energy is given as a fraction of the cohesive energy, which is equal to $0.11 E_{\text{coh}}$ in an amorphous polymer. Finally, the thermal energy of the system, H_T is achieved by considering the polymer chain as being a strong chain oscillator in a weak 3-dimensional field, using the Tarasov modification of the Debye theory.^{1,5,7} From the equation of state and the Tarasov equation, it is possible to calculate a number of volumetric properties of a polymer such as the heat capacity, C_p , and the thermal expansion coefficient α (where R is the molar gas constant), given in eqs. (2) and (3).

$$C_p = NR \frac{\left(\frac{6.7 T}{\theta_1} \right)^2}{1 + \left(\frac{6.7 T}{\theta_1} \right)^2} \quad (2)$$

$$\alpha = \frac{1.38}{E_{\text{coh}}} \cdot \frac{C_p}{R} \quad (3)$$

An expression for the elastic bulk modulus is obtained by differentiating the potential function in the equation of state with respect to volume, which simplifies to:

$$B_e = 18 \frac{E_{\text{total}}}{V} \quad (4)$$

To quantify the full viscoelastic response of a polymer, expressions relating the energy dissipation at the molecular level are defined, from which the bulk and Young's moduli are calculated. The loss processes break down into thermomechanical losses and loss peaks due to transition events. The thermomechanical loss arises from mechanical energy being transferred irreversibly into heat because of changes to the thermal parameters. It is given by:

$$\tan \delta = -A \frac{dB}{dT} = -\frac{1.5 \times 10^5 L}{\theta_1 M} \cdot \frac{dB}{dT} \quad (5)$$

where A is the proportionality constant, L is the length of the polymer chain mer unit, and M is the molecular weight. The transition events in polymers, T_β and T_g , are attributed to the peaks in loss tangent, where new degrees of freedom are activated. The glass transition is related to the Born elastic instability criterion where the second differential of the Lennard-Jones function tends to zero.³ The beta transition, however, is believed to be associated with the onset of torsional motion in main chain aromatic rings when present in the polymer backbone.^{2,3} Predictions for these two transition temperatures with their associated cumulative loss tangents, $\tan \Delta_g$ and $\tan \Delta_\beta$, are given by eqs. (6-9):

$$T_g = 0.224 \theta_1 + 0.0513 \frac{E_{\text{coh}}}{N} \quad (6)$$

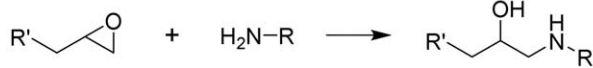
$$\tan \Delta_g = 0.0085 \frac{E_{\text{coh}}}{N_c} \left(\frac{N-3X}{N} \right) \quad (7)$$

$$T_\beta = \frac{-\Delta H_\beta}{R \ln \left(\frac{r}{2\pi f} \right)} \left(\frac{N}{N-3X} \right) \quad (8)$$

$$\tan \Delta_\beta = 25 \frac{\Delta N_\beta}{N_c} \quad (9)$$

Here ΔH_β is the activation energy of the β -transition (which for aromatic rings is the energy associated with phenyl ring flips),

Primary Epoxy-Amine Reaction



Secondary Epoxy-Amine Reaction

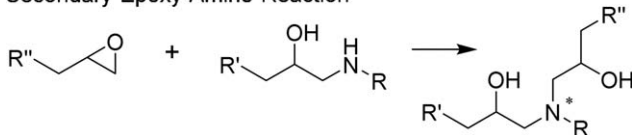


Figure 1. Epoxy reaction mechanism.

r is the applied strain rate and f is the characteristic vibrational frequency of the polymer chain. It is given by:

$$f = \frac{k\theta_1}{h} \quad (10)$$

where k is the Boltzmann constant and h is Planck's constant. By combining the loss processes with the elastic bulk modulus, expressions for the bulk and Young's modulus are now given by:

$$B = B_e \left(1 - \frac{\Delta N_\beta(T)}{N_c} \right) \left(1 - \frac{\Delta N_g(T)}{N} \right) \quad (11)$$

$$E_\beta = B_e \exp \left(- \frac{\int_0^T \tan \delta_\beta dT}{AB_e} \right) \quad (12)$$

$$E = \frac{E_\beta}{\left(1 + \int_0^T \tan \delta_g dT \right)^2} \quad (13)$$

where E_β is the Young's modulus below the glass transition and E is the Young's modulus through and above the glass transition. The combination of the bulk and tensile (Young's) moduli then give a prediction for the Poisson's ratio of the form:

$$\nu = 0.5 \left(1 - \frac{E}{3B} \right) \quad (14)$$

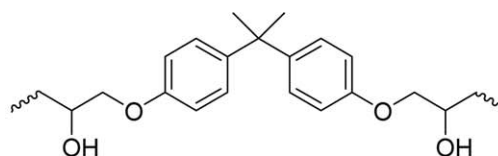
From the volumetric and dynamic mechanical properties, the stress-strain predictions are now made as a function of temperature as a dummy variable.

$$\varepsilon = \int_{T_0}^T \alpha_\sigma dT \quad (15)$$

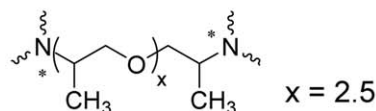
$$\sigma_t = \int_{T_0}^T E_\sigma \alpha_\sigma dT \quad (16)$$

$$\sigma_c = \frac{\sigma_t}{2\nu_\sigma} \quad (17)$$

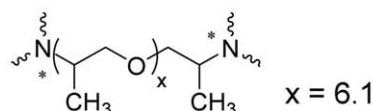
As an extension of these stress and strain equations, it is possible to estimate the stress relaxation rate with strain, by assuming that yield is an activated rate process with an activation



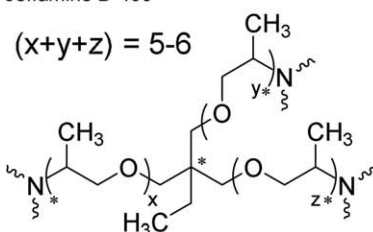
DGEBA (diglycidyl ether of bisphenol-A)



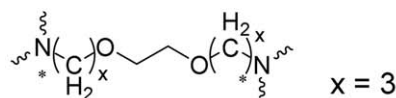
Jeffamine D-230



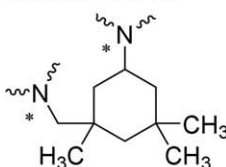
Jeffamine D-400



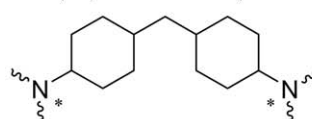
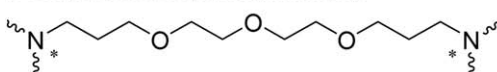
Jeffamine T-403



Jeffamine EDR-176



IPDA (isophorone diamine)

PACM (bis *p*-aminocyclohexyl methane)

TTD (4,7,10-trioxatridecane-1,13-diamine)

Figure 2. Cured chemical structures of DGEBA and the liquid amines used in this study. Here * denotes a crosslink point.

energy.² It assumes that there is effectively a lower limiting yield stress at infinitely low strain rates, σ_{y0} , which the post-yield stress must relax down to at any given strain rate. The post-yield strain relaxation is therefore given by:

Table I. GIM Parameters for the Cured Epoxy and Amine Mer Units

Mer unit	<i>N</i>	<i>E_{coh(P)}</i> (J mol ⁻¹)	<i>E_{coh(B)}</i> (J mol ⁻¹)	<i>V_w</i> (cc mol ⁻¹)	<i>M</i>	<i>L</i> (Å)	<i>N_c</i>	<i>N_β</i>	X-links
DGEBA	24	13,5700	n/a	192.92	342	15.48	46	6	0
D-230	30	81,000	66,858	130.26	226	11.40	30	0	2
D-400	58.8	15,2280	12,9879	261.16	426	23.90	58.8	0	2
T-403	61	16,2900	13,8143	270.35	434	15.35	41.33	0	4
EDR-176	24	66,600	56,811	99.84	172	14.46	24	0	2
IPDA	12	59,000	46,783	104.23	164	6.90	24	0	2
PACM	14	68,500	60,006	124.83	206	10.50	42	0	2
IPDA + TTD	21	70,450	58,939	159.77	190	11.87	27	0	2

$$\sigma_y(\epsilon) = \sigma_{y0} + (\sigma_{yr} - \sigma_{y0}) \exp\left(-\left(\frac{\epsilon_{ya}}{\epsilon}\right)^2\right) \quad (18)$$

where σ_{yr} is the yield stress at a given strain rate r and ϵ_{ya} is the activation strain for yield.

Parameterization of GIM

As indicated above, GIM requires a number of input parameters, which must be assigned based on a reasonable assumption of the chemical structure of the polymer being modeled.¹⁻³ For simple linear polymers, this is a straightforward task as the structure is known, whereas for thermosetting polymers, knowledge of the reaction mechanisms, and crosslink density are required to estimate the likely network structure. For epoxy resins, the epoxy and amine monomers typically react to form a three dimensional polymer network via two main reactions. The first reaction is a primary amine reacting with an epoxy ring and the second reaction is when the resultant secondary amine reacts with another epoxy ring. Both reactions can be seen in Figure 1.

For the purpose of this study, and as a first approximation, the network structure has been assumed to be the result of total consumption of reactive hydrogen to form an ideal 100% cross-linked network, to compare with fully cured experimental specimens. The GIM parameters are therefore assigned for the ring opened form of the DGEBA epoxy along with the amines used in this study, with the network structures shown in Figure 2. The required parameters for GIM predictions are as follows:¹

- Molar mass, *M*
- Cohesive energy, *E_{coh}*
- Van der Waals volume, *V_w*
- Degrees of freedom, *N*
- Degrees of freedom in chain axis, *N_c*
- Degrees of freedom active in the beta transition, *N_β*
- Length of mer unit, *L*
- Debye temperature parallel to the chain axis (chain stiffness), θ_1
- Activation energy, ΔH_β
- Theoretical maximum number of crosslinks, *X*

Table I shows all of the parameters for the epoxy and amine network fragments. The parameters *M*, *E_{coh}*, *V_w*, and *N* are assigned using group contribution tables outlined by Porter,¹ with the exception of the —CH(OH)— segment found in DGEBA. For this structural unit, the refined parameters for *E_{coh}* and *N* proposed by Foreman et al.² were used, which includes a 10 kJ mol⁻¹ increment in *E_{coh}* to account for hydrogen bonding. In network polymers, the value of *N* must be corrected for crosslinking by removing three degrees of freedom at each crosslink point. The assignment of *N_c* can be calculated using simple rules found in Porter,¹ while it is assumed in the first instance that *N_β* takes a value equal to the degrees of freedom for the phenyl rings in each network fragment. The length of the mer unit, *L*, can be found via simple molecular modeling techniques. In this work, the average length of each mer unit was found by performing molecular dynamics simulations for 100 ps at 300 K using HyperChem (Hypercube) software. These simulations were performed after initial geometry minimization to an RMS gradient of 0.001 kcal Å⁻¹ mol⁻¹, using the semi-empirical AM1 method.¹⁶ The Debye temperature parallel to the chain axis, θ_1 , is a measure of the backbone stiffness of a polymer as it is related to the vibrational frequencies of the groups in the chain. For polymers with aromatic rings in the backbone, it is taken to be 550 K.¹

In this study, an alternative value for the cohesive energy, *E_{coh(B)}* (as opposed to *E_{coh(P)}* using Porter's rules), is assigned using Polymer Design Tools (DTW Associates), a molecular modeling software package that allows the estimation of a number of properties as a function of temperature using the Bicerano method,¹⁷ so that the effect of the parameterization method on the GIM predictions can be established. As the GIM predictions for the glass transition temperature are solely dependent on

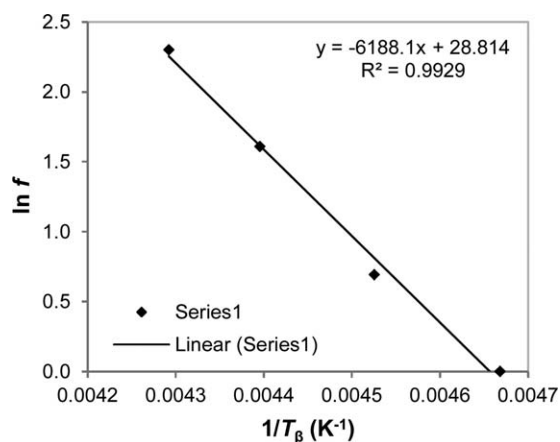


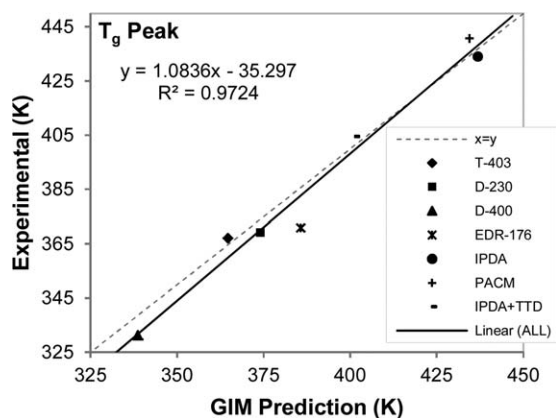
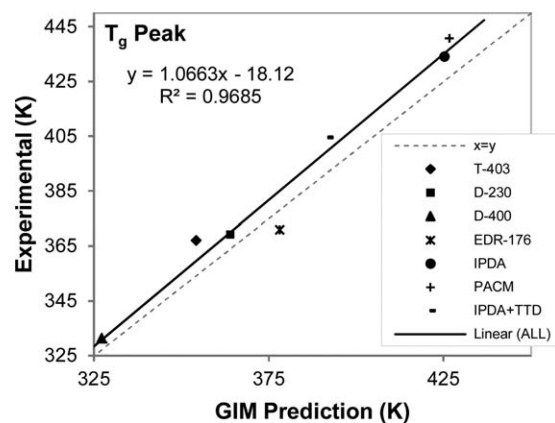
Figure 3. Example Arrhenius plot for calculating the activation energies of DGEBA cured with D-230.

Table II. Values of T_g Experimental and GIM Predictions using Two Different Methods of Assigning the Cohesive Energy

Resin	Exp. T_g (K)	GIM T_g prediction (K)	
		Using $E_{coh(P)}$	Using $E_{coh(B)}$
DGEBA/D-230	367	365	354
DGEBA/D-400	369	374	364
DGEBA/T-403	331	339	327
DGEBA/EDR-176	371	386	378
DGEBA/IPDA	434	437	425
DGEBA/PACM	441	434	427
DGEBA/IPDA + TTD	404	401	392
Pearson's r	-	0.986	0.985
P -value	-	<0.001	<0.001

E_{coh} , N , and θ_1 [see eq. (6) above], these predictions can provide a good measure of how well the cohesive energy parameter is assigned.

The final parameter, which needed assigning, is the activation energy, ΔH_β , which is used to predict the peak temperature of the subambient beta transition, T_β present in epoxy resins. This beta transition in amorphous polymers is associated with the dissipation of energy due to crankshaft or torsional motion in the polymer backbone or side chains. For polymers with phenyl rings in the backbone, it is the torsional motion between neighbouring phenyl rings that is believed to dominate the beta transition,^{2,3} and so an activation energy is required for the bisphenol-A epoxy used in this study. Work by Porter and Gould,³ and Foreman et al.² both used a value of 44 kJ mol⁻¹ for ΔH_β for structures with a bisphenol-A backbone; an attempt is made here to determine whether this value is the best for the resins used in this work, or whether a different value is more suitable for the specific environments of the resins used here. An empirical value for the activation energy is also derived with the aid of experimental multifrequency DMA test results and compared with the assumed values.

**Figure 4.** Experimental results plotted against GIM predictions for the peak glass transition temperature using E_{coh} determined by group contribution tables in Porter,¹ at a frequency of 1 Hz. Dashed line shows $x = y$.**Figure 5.** Experimental results plotted against GIM predictions for the peak glass transition temperature using E_{coh} determined by the Bicerano method,¹⁷ at a frequency of 1 Hz. Dashed line shows $x = y$.

EXPERIMENTAL

In contrast to typical aerospace amines, the liquid amines used here are aliphatic and cycloaliphatic compounds that react with Epikote 828 (DGEBA) at room temperature. Consequently, they were mixed vigorously at room temperature in a Synergy Devices DAC 250 FVZ-K Speedmixer for 5–10 min before degassing in a vacuum chamber until any bubbles present had been removed. Once degassed, the resins were poured into suitable molds to create resin plaques (50 × 50 × 6 mm) and cylinders (50 × 13 mm), from which the test specimens for DMA and compressive stress-strain testing, respectively, could be machined after cure. The cure was performed at room temperature (295 K) for 3 days followed by a 2 h postcure, with an initial ramp rate of 1 K min⁻¹, at 373 K (100°C) for the Jeffamines and 423 K (150°C) for IPDA, PACM, and IPDA + TTD.

The cured rectilinear specimens for DMA testing were cut on a Buehler IsoMet 5000 precision saw to dimensions of around 50 × 6 × 2 mm (length × width × thickness), which were tested in single cantilever mode with a gauge length of 40 mm and displacement amplitude of 10 μm, on a Mettler Toledo DMA/SDTA861e. These test conditions and sample geometry were carefully chosen to ensure the most accurate Young's modulus measurements according to ISO 6721. The tests were carried out as a multifrequency experiment at 1, 2, 5, and 10 Hz, and specimens were heated at a rate of 2 K min⁻¹ from 173 K (-100°C) to above the glass transition, so that both the glass transition and the beta transition could be determined. One sample of each resin was tested, with the exception of DGEBA cured with EDR-176, for which three repeats were performed to ensure repeatability between tests. To calculate the empirical activation energies from the experimental multifrequency DMA tests, the Arrhenius equation defined below can be used as the beta transition is a frequency dependent, thermal event.

$$\ln f = \ln A - \frac{\Delta H_\beta}{RT_\beta} \quad (19)$$

Here, the activation energy, ΔH_β , is measured from an Arrhenius plot of $\ln f$ versus $1/T_\beta$ where f is the frequency of the DMA experiment, T_β is the peak temperature of the beta

Table III. Comparisons Between Experimental T_{β} and GIM Predictions Using Three Different Methods of Assigning the Activation Energy; the Literature Value of 44 kJ mol^{-1} ,³ the Average Calculated 50 kJ mol^{-1} and the Empirically Calculated Activation Energies

Resin	Exp. T_{β} (K)	GIM T_{β} prediction using different ΔH_{β} (K)		
		44 kJ mol^{-1}	50 kJ mol^{-1}	Emp. ΔH_{β}
DGEBA/D-230	214	190	217	222
DGEBA/D-400	205	186	212	232
DGEBA/T-403	211	193	220	209
DGEBA/EDR-176	225	191	218	248
DGEBA/IPDA	217	195	222	310
DGEBA/PACM	235	194	222	245
DGEBA/IPDA + TTD	220	192	219	330
Pearson's r	-	0.588	0.656	0.308
P -value	-	0.165	0.110	0.502

transition, R is the molar gas constant, and $\ln A$ is the pre-exponential factor and the y -intercept; the activation energy is calculated from the gradient of the plot. Figure 3 shows an example Arrhenius plot for DGEBA cured with D-230.

The cured cylindrical specimens, for the compressive stress-strain characterization, were machined on a lathe to a nominal diameter of 12 mm and length of 18 mm, giving a length-to-diameter ratio of 3 : 2. This length-to-diameter ratio was chosen to minimize the possibility of buckling and/or the effects of frictional constraint, which occur at high and low aspect ratios, respectively.¹⁸ One 2 mm uniaxial strain gauge was bonded along the length of each of the cylindrical specimens, so that the axial strain could be measured and recorded using a data logger. Three specimens of each resin were tested through yield using an Instron 5582 testing machine with a load cell of 100 kN at a cross-head displacement rate of 1 mm min^{-1} at room temperature, to ensure repeatability. When analyzing the results, yield was defined as the point of maximum stress (or the point of inflexion for DGEBA cured with PACM as it does not go through a maximum).

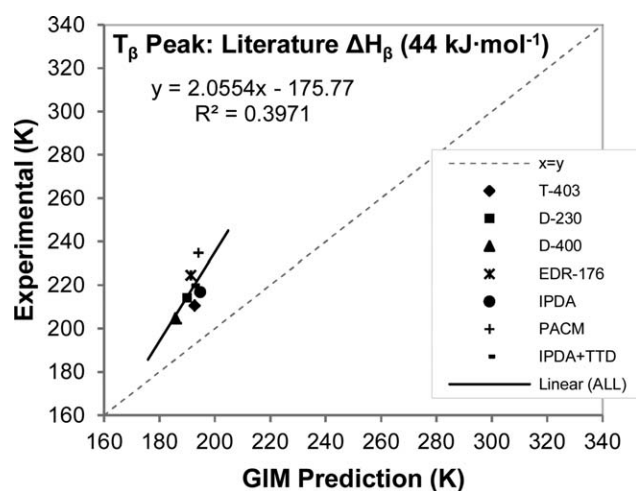


Figure 6. Experimental results plotted against GIM predictions for the beta transition temperature using a literature value of 44 kJ mol^{-1} for activation energy,³ at a frequency of 1 Hz. Dashed line shows $x = y$.

In addition to the DMA and compressive stress-strain testing, all cured and uncured specimens were analyzed by differential scanning calorimetry (DSC) to establish the degree of cure so that this empirical value could be used in the GIM predictions for each resin system. It was found that there were no residual exotherms for all of the cured specimens, and therefore the degree of cure used in the GIM predictions was taken to be 100% to match this.

RESULTS AND DISCUSSION

Dynamic Mechanical Analysis

The results for the peak glass transition temperature, at a frequency of 1 Hz, for the liquid amine cured resins, as measured experimentally from the tan-delta DMA curve, and the predicted values using GIM are shown in Table II and illustrated in Figures 4 and 5. It can be seen that there is a strong correlation between the experimental results and both sets of predictions using $E_{\text{coh(P)}}$ and $E_{\text{coh(B)}}$, respectively. There is also <4% difference between all predicted and experimental values, with only small differences in the predicted values.

However, when comparing the experimental data for the peak beta transition temperature with the GIM predictions, at a frequency of 1 Hz, assuming an activation energy of 44 kJ mol^{-1} ,^{2,3} it can be seen that the experimental values do not

Table IV. Required GIM Activation Energies to Give the Correct T_{β} Predictions Along with the Empirically Calculated Activation Energies from the Multifrequency DMA Experiments

Resin	Required ΔH_{β} (kJ mol^{-1})	Empirical ΔH_{β} (kJ mol^{-1})
DGEBA/D-230	50	51
DGEBA/D-400	48	55
DGEBA/T-403	49	48
DGEBA/EDR-176	52	57
DGEBA/IPDA	49	70
DGEBA/PACM	53	56
DGEBA/IPDA + TTD	50	76

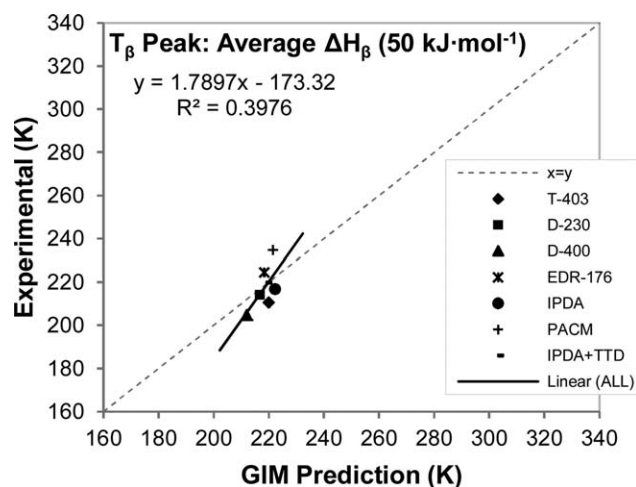


Figure 7. Experimental results plotted against GIM predictions for the beta transition temperature using an average required value in GIM of 50 kJ mol^{-1} , at a frequency of 1 Hz. Dashed line shows $x = y$.

agree with the GIM predictions, with the experimentally measured temperatures being significantly higher than the GIM predictions (see Table III and Figure 6). It was therefore decided to investigate if a different value for the activation energy could be used for all resin systems, or whether it was possible to use empirically calculated activation energies from the multifrequency DMA experiments, to give predictions that more closely match the experimental data.

To determine a single activation energy that could be used for the seven resins in this study, the experimental T_{β} values were used in GIM to back-calculate what the required GIM activation energies were, with the results shown in Table IV. These results show a small variation in the required activation energies from 48 to 53 kJ mol^{-1} with a mean value and standard deviation of $50 \pm 2 \text{ kJ mol}^{-1}$. This value of average activation energy has been used in the GIM predictions (rather than the 44 kJ

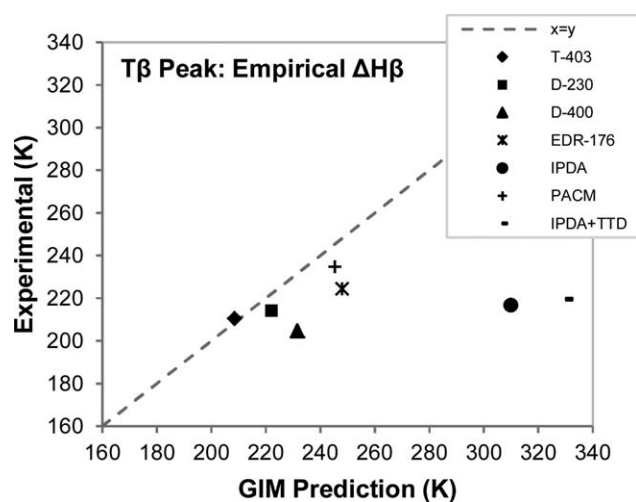


Figure 8. Experimental results plotted against GIM predictions for the beta transition temperature using the empirically derived activation energies from the experimental multifrequency DMA experiments, at a frequency of 1 Hz. Dashed line shows $x = y$.

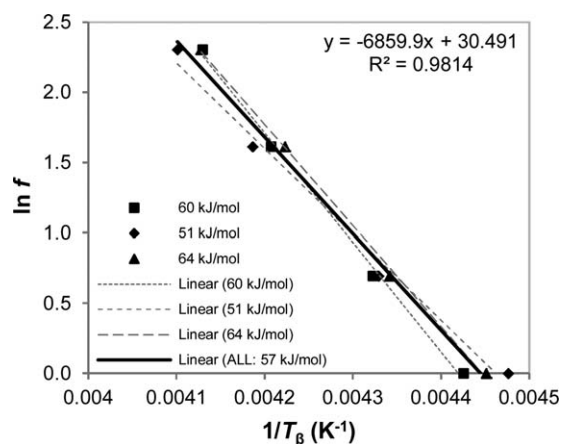


Figure 9. Arrhenius plot for calculating the activation energies of three repeats of DGEBA cured with EDR-176.

mol^{-1} value), with the experimental and GIM predicted values shown in Figure 7. Using this method, predictions for all resins are within 6% of the experimental values, which can be seen in Table III along with the predictions using both 44 kJ mol^{-1} and the empirically calculated activation energies.

The experimental results for T_{β} plotted against the GIM predictions using these empirically derived activation energies are shown in Figure 8. There appears to be a reasonably good correlation between the GIM predictions and the experimental data for three of the resins, namely DGEBA cured with T-403, D-230, and PACM, where predictions are within 4% of the experimental values. There is, however, a much poorer correlation between predictions and experimental data for DGEBA cured with D-400 and EDR-176, and little or no agreement for IPDA and IPDA + TTD, which suggests that there is an issue with IPDA. It is possible that this relates to the rather compact nature of the chemical structure of IPDA compared to the other amines used in this study, which are typically long and flexible. This could make it more difficult for IPDA to fully react, as once partially reacted, its mobility will be greatly reduced making it difficult to meet an unreacted epoxy group.

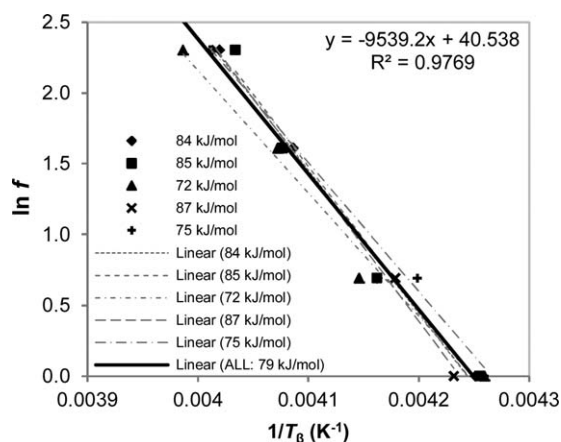


Figure 10. Arrhenius plot for calculating the activation energies of five repeats of DGEBA cured with EDR-176 after drying in a vacuum oven at 343 K until constant weight.

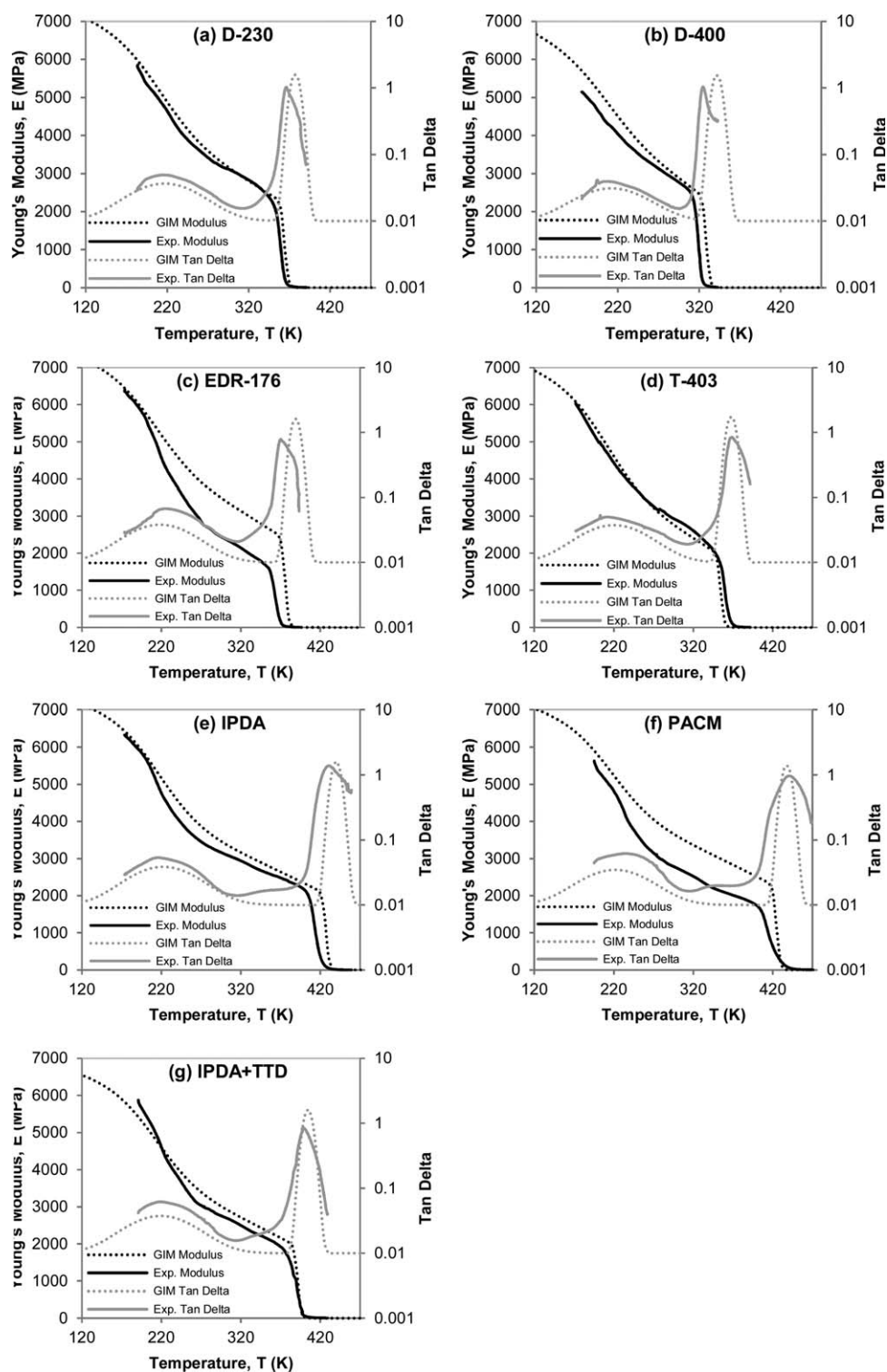


Figure 11. Overlays of the experimental DMA curves with the GIM predictions using an activation energy of 50 kJ mol^{-1} , at a frequency of 1 Hz, for DGEBA cured with (a) D-230; (b) D-400; (c) EDR-176; (d) T-403; (e) IPDA; (f) PACM; and (g) IPDA + TTD.

Interrogation of the experimental data for DGEBA cured with EDR-176, found that for a set of three repeats, there was a relatively large variation in the calculated activation energy, between 51 and 64 kJ mol^{-1} with a mean of 57 kJ mol^{-1} , as can be seen from the Arrhenius plot in Figure 9. Using these

different, empirically determined activation energies in the GIM predictions, it was found that an increase of just 1 kJ mol^{-1} in ΔH_{β} gives a predicted increase of 4.3 K in T_{β} for DGEBA cured with EDR-176, meaning the GIM predictions using these upper and lower activation energies will vary over

Table V. Values of Yield Stress from Experimental and GIM Predictions Using Two Different Methods of Assigning the Cohesive Energy, with All Predictions Made Using the Average Activation Energy of 50 kJ mol⁻¹

Resin	Experimental σ_y (MPa)				GIM σ_y prediction (MPa)	
	#1	#2	#3	Ave.	Using $E_{\text{coh(P)}}$	Using $E_{\text{coh(B)}}$
DGEBA/D-230	87	87	84	86	125	108
DGEBA/D-400	64	64	64	64	107	85
DGEBA/T-403	80	80	80	80	99	83
DGEBA/EDR-176	74	75	75	75	148	135
DGEBA/IPDA	116	116	117	116	151	135
DGEBA/PACM	115	115	114	115	170	158
DGEBA/IPDA + TTD	95	94	94	94	124	111
Pearson's <i>r</i>				-	0.724	0.733
<i>P</i> -value				-	0.066	0.061

as much as 64 K. This highlighted the sensitivity of the GIM T_β predictions to the activation energy, and prompted further investigation into the derivation of the empirically determined activation energies.

With moisture known to affect the transition temperatures of polymers, it was decided to perform a set of five repeat experiments for this resin system after drying in a vacuum oven at 343 K (70°C) until constant weight, to see if this influenced the results. These new results, shown in Figure 10, gave an average T_β peak temperature of 235 ± 1 K at a frequency of 1 Hz, which can be compared with the value of 225 ± 1 K for the previous set, along with average activation energy of 79 kJ mol⁻¹ compared with the previous value of 57 kJ mol⁻¹. Using this new activation energy has the result of increasing the GIM predicted T_β peak at 1 Hz from 248 to 345 K, which is much further away from the experimental value of 225 K. Furthermore, there was still a 15 kJ mol⁻¹ range of calculated activation energies from this carefully dried set of DGEBA cured with EDR-176. It is possible that this variation could be reduced by increasing the range of frequencies tested by one or two orders of magnitude, as current tests were limited to frequencies between 1 and 10 Hz.

In addition to this large variation in empirically calculated activation energies for a single resin system, it is possible that there is an effect due to thermal history on the measured activation energies. It can be seen that the effect of drying EDR-176 specimens at elevated temperature has caused an increase in the empirically calculated activation energy of 22 kJ mol⁻¹. When referring back to Table IV it can be seen that two out of the three resins (namely DGEBA cured with IPDA and IPDA + TTD) cured at the higher temperature of 423 K, as opposed to 373 K for the Jeffamines, have much higher empirically calculated activation energies. It is possible that the higher temperatures these resins have seen have induced a higher level of strain into the experimental specimens affecting the relaxation process, and ultimately the empirically calculated activation energies.

Due to the shortcomings of the empirically calculated activation energies, comparisons of the predicted DMA curves with the experimental data at a frequency of 1 Hz are shown in Figure 11, using the average activation energy of 50 kJ mol⁻¹ for these predictions, for which T_β is predicted reasonably well. It can be seen that, in general, there is very good agreement between the predictions and the experimental data for the majority of these resins, for both

Table VI. Values of Yield Strain from Experimental and GIM Predictions Using Two Different Methods of Assigning the Cohesive Energy, with All Predictions Made Using the Average Activation Energy of 50 kJ mol⁻¹

Resin	Experimental ϵ_y				GIM ϵ_y prediction	
	#1	#2	#3	Ave.	Using $E_{\text{coh(P)}}$	Using $E_{\text{coh(B)}}$
DGEBA/D-230	0.051	0.048	0.044	0.048	0.084	0.085
DGEBA/D-400	0.033	0.025	0.029	0.029	0.079	0.075
DGEBA/T-403	0.057	0.050	0.047	0.052	0.080	0.081
DGEBA/EDR-176	0.061	0.063	0.067	0.063	0.087	0.086
DGEBA/IPDA	0.081	0.088	0.080	0.083	0.097	0.095
DGEBA/PACM	0.101	0.103	0.097	0.100	0.095	0.095
DGEBA/IPDA + TTD	0.073	0.068	0.080	0.073	0.091	0.088
Pearson's <i>r</i>				-	0.922	0.951
<i>P</i> -value				-	0.003	0.001

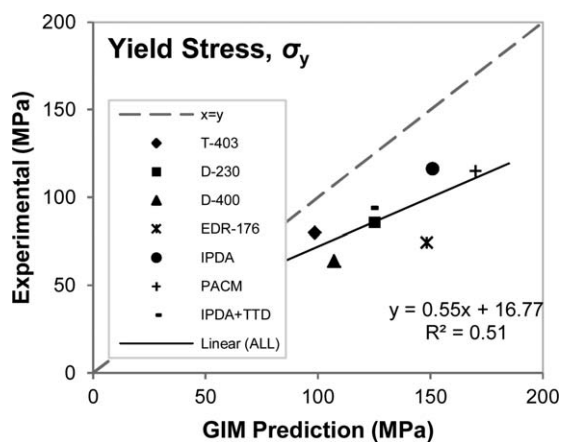


Figure 12. GIM predicted versus experimental data for the compressive yield stress at a strain rate of 0.001 s^{-1} , using $E_{\text{coh}(P)}$. Dashed line shows $x = y$.

modulus and tan-delta curves. There are, however, significant discrepancies between the experimental and predicted modulus values for DGEBA cured with EDR-176 and PACM [Figure 11(c,f)]. Work by Vanlandingham et al.¹⁹ on DGEBA cured with PACM found that this resin system exhibits a two-phase microstructure consisting of a hard microgel phase and a soft phase of unreacted and/or partially reacted material. This could explain the reason for the experimental modulus of this resin system being significantly lower than the GIM prediction, and EDR-176 may behave in a similar fashion. It is clear that in both cases, the model predictions with the assumptions made on network structure do not match what is observed experimentally, and therefore further insight into the network structure of these resins is needed for accurate predictions to be made in terms of modulus.

Compressive Stress-Strain Response

A comparison between experimental data and the GIM predictions for the compressive yield stress and strain are tabulated in Tables V and VI and shown graphically in Figures 12 and 13 (for predictions using $E_{\text{coh}(P)}$). The GIM predictions were made

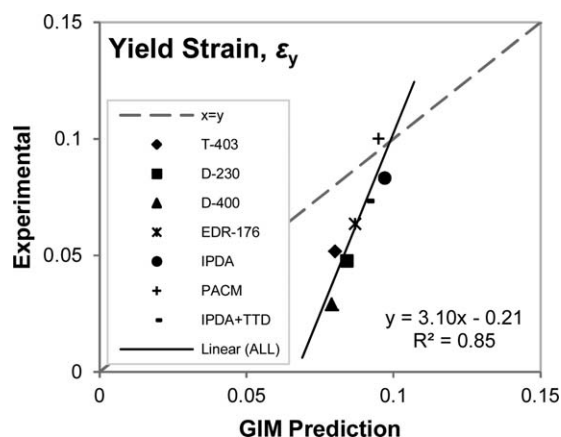


Figure 13. GIM predicted versus experimental data for the compressive yield strain at a strain rate of 0.001 s^{-1} , using $E_{\text{coh}(P)}$. Dashed line shows $x = y$.

using the average activation energy of 50 kJ mol^{-1} , to match the comparative results given in Figure 11 for the DMA traces.

It can be seen that for the yield stress there is a reasonable correlation between experimental and predicted data using Porter's E_{coh} , although the GIM does, however, over-predict the yield stress values by an average of 49%. When the cohesive energy was assigned using the molecular modeling techniques of Bicerano¹⁷ instead of using the group contribution tables in Porter,¹ the predicted yield stress values were typically lower and closer to the experimental data, although still higher by an average of 31%. The reason for this general over-prediction of the yield stress could be due to a number of factors. First, the epoxy used in this study is Epikote 828, which contains a proportion of oligomers and dimers, which will act as plasticizers in the cured resin, therefore lowering the experimental yield stress. Another possibility for the over-prediction of the yield stress is due to the GIM predictions being based on the assumption of a 100% crosslinked network, with full consumption of epoxy and amine groups, to match degree of cure data generated by DSC. In reality, it is well known that epoxy resins only cure to around 90%, as beyond this, the network structure is constrained with little mobility, making it difficult to reach full conversion. While the DSC traces showed no residual exotherm for all the resins tested in this work, this means is that there were no unreacted epoxy and amine groups with close enough proximity to react, but there could be a number of unreacted groups in the network, acting as plasticizers.

While the yield stress predictions are generally over-predicted, it is clear that the GIM predictions for the yield strains appear to be restricted to a very small range of values between 0.075 and 0.097. This is in contrast to the experimental values for this class of resins, which cover a much broader range from 0.029 to 0.100. There is however a linear relationship with very good correlation between the predicted and experimental data as shown in Figure 13. These results indicate that there is either a limitation in the GIM predictions or the experimental measurement, or possibly a combination of the two. In terms of the GIM predictions it is possible there is a free volume effect that is not correctly accounted for in the GIM model at present. With regards to the experimental data, it is likely that the low yield strains seen could be due to slight barrelling of the specimens, where the centre of the specimen (which the strain gauge was bonded to) was around $300 \mu\text{m}$ ($\sim 2.5\%$) thicker in diameter than either end, causing a small amount of localised rather than general deformation. When looking more closely at the experimental data, it can be seen that the resins cured with the amines with long backbones, such as Jeffamine D-400, have very low yield strains due to the large amount of flexibility allowing for the reordering of network segments at low strains. Resins cured with IPDA and PACM however give much higher yield strains, which can be attributed to the more compact nature of these amines, allowing less movement of network segments at low strain levels.

While the comparisons between the GIM predictions and experimental data for the yield characteristics of these resins have some limitations, it can be seen from the compressive stress-strain curves that the predictions are typically in good

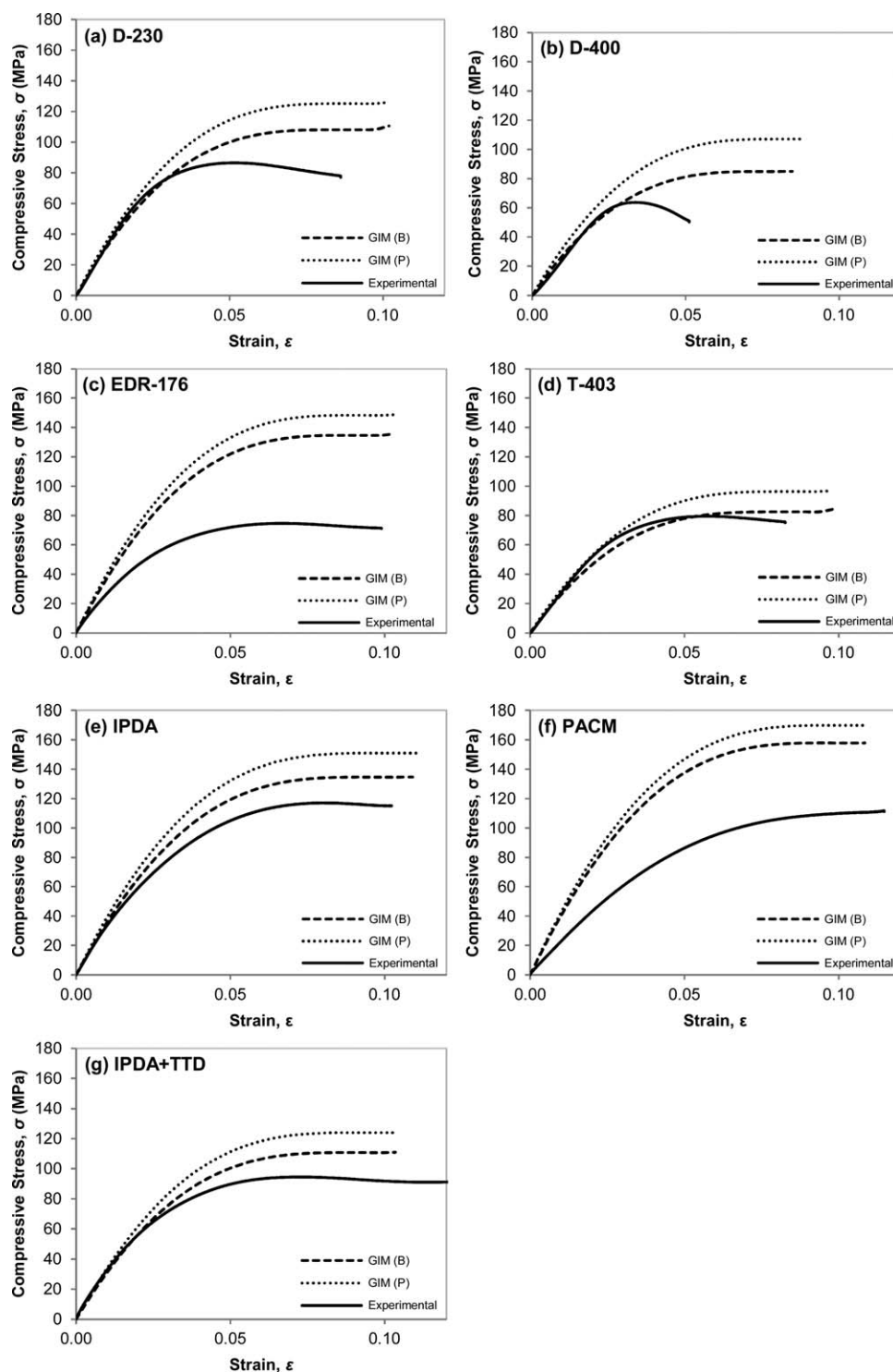


Figure 14. Overlays of the experimental compressive stress-strain curves with the two GIM predictions using $E_{\text{coh}(P)}$ and $E_{\text{coh}(B)}$ and an activation energy of 50 kJ mol^{-1} , at a strain rate of 0.001 s^{-1} , for DGEBA cured with (a) D-230; (b) D-400; (c) EDR-176; (d) T-403; (e) IPDA; (f) PACM; and (g) IPDA + TTD.

agreement with the experimental results for the low strain portions of the stress-strain curves (see Figure 14). For this region of the stress-strain curves, only the predictions for DGEBA cured with EDR-176 and PACM do not agree well with the experimental data for any region of the stress-strain curves. It

can also be seen from the comparison of the predicted and experimental DMA modulus curves that these two resin systems also have larger variation between experimental and predicted modulus values. This suggests that the assumptions made on network structure when assigning the GIM parameters for these

two resins does not accurately match what is obtained experimentally, as discussed in the results for the DMA curves. It should be noted that the stress-strain predictions in GIM, particularly for yield, are complex and dependent on the majority of input parameters, and so accurate predictions can be difficult to obtain when making assumptions on network structure. This is in contrast to the predictions for the glass transition temperature, which for aromatic resins, where θ_1 is a constant, is only dependent on E_{coh} and N .

CONCLUDING REMARKS

The results of the characterization of a number of liquid amine cured epoxy resins by DMA and compressive stress-strain tests, have been compared to predictions made using GIM, with varying degrees of success. In this work, broad assumptions for the predictions, based on the formation of a 100% crosslinked network were made, to see if accurate predictions could be made without the need for more complex modeling of individual moieties, such as that employed by Liu et al.⁸

Comparative results for T_g are excellent, with the predictions agreeing very well with the experimental data, using two different methods for the assignment of the cohesive energy. For the T_β predictions, the initial value of 44 kJ mol^{-1} for the activation energy used in GIM, which was taken from previous literature, was found to under-predict T_β , suggesting these liquid amine cured epoxies required a higher activation energy. The revised value of 50 kJ mol^{-1} gave predictions that agree well with experimental data. Attempts were also made to calculate empirical activation energies for these resins from multifrequency DMA tests, although there appeared to be too much variation in these measured activation energies and potentially too much influence from experimental factors such as thermal history affecting these results.

In terms of the stress-strain characteristics, the yield stress is generally over-predicted, which can be attributed to the assumption of a 100% crosslinked network, which in reality is likely to be closer to 90%, along with the presence of oligomers and dimers in the Epikote 828 resin, which act to reduce the yield stress by plasticizing the network. Comparative data for the yield strain, however, show a strong correlation, but there is a much broader range of yield strains seen experimentally than predicted.

The overriding conclusions from this work are twofold. First, the GIM predictions can be very sensitive to certain parameters, where small differences in these inputs can result in large differences in the predictions, such as the effect of cohesive energy on yield stress. As a result, it is necessary to be conscious of which parameters drive the predictions for each property. Second, it is important to have a more in depth knowledge of the network structure of the resins being modeled as basic assumptions are not generally adequate enough for accurate predictions of complex properties such as the stress-strain characteristics,

although they are good enough for the glass transition temperature. For the resins used in this study, this is particularly the case for DGEBA cured with EDR-176 and PACM, for which the T_g predictions are good and the stress-strain predictions poor in comparison to the experimental data.

ACKNOWLEDGMENTS

This work was carried out as part of the University of Surrey Engineering Doctorate (EngD) Programme in Micro- and NanoMaterials and Technologies with Hexcel Composites as the sponsoring company and funded by the EPSRC.

REFERENCES

1. Porter, D. *Group Interaction Modelling of Polymer Properties*; Marcel Dekker: New York, **1995**.
2. Foreman, J. P.; Porter, D.; Behzadi, S.; Jones, F. R. *Polymer* **2008**, *45*, 5588.
3. Porter, D.; Gould, P. J. *Int. J. Solids Struct.* **2009**, *46*, 1981.
4. Porter, D. *Adv. Perform. Mater.* **1996**, *3*, 309.
5. Tilbrook, D. A.; Pearson, G. J.; Braden, M.; Coveney, P. V. *J. Polym. Sci. Part B: Polym. Phys.* **2003**, *41*, 528.
6. Porter, D.; Gould, P. J. *J. Phys. IV.* **2006**, *134*, 373.
7. Gumen, V. R.; Jones, F. R.; Attwood, D. *Polymer* **2001**, *42*, 5717.
8. Liu, H.; Uhlherr, A.; Bannister, M. K. *Polymer* **2004**, *45*, 2051.
9. Foreman, J. P.; Porter, D.; Behzadi, S.; Travis, K. P.; Jones, F. R. *J. Mater. Sci.* **2006**, *41*, 6631.
10. Foreman, J. P.; Behzadi, S.; Porter, D.; Curtis, P. T.; Jones, F. R. *J. Mater. Sci.* **2008**, *43*, 6642.
11. Foreman, J. P.; Behzadi, S.; Tsampas, S. A.; Porter, D.; Curtis, P. T.; Jones, F. R. *Plast. Rubber Compos.* **2009**, *38*, 67.
12. Foreman, J. P.; Porter, D.; Behzadi, S.; Curtis, P. T.; Jones, F. R. *Compos. A* **2010**, *41*, 1072.
13. Foreman, J. P.; Behzadi, S.; Porter, D.; Jones, F. R. *Philos. Mag.* **2010**, *90*, 4227.
14. Ersoy, N.; Garstka, T.; Potter, K.; Wisnom, M. R.; Porter, D.; Clegg, M.; Stringer, G. *Compos. A* **2010**, *41*, 401.
15. Ersoy, N.; Garstka, T.; Potter, K.; Wisnom, M. R.; Porter, D.; Stringer, G. *Compos. A* **2010**, *41*, 410.
16. Dewar, M. J. S.; Zoebisch, E. G.; Healy, E. F.; Stewart, J. J. P. *J. Am. Chem. Soc.* **1985**, *107*, 3902.
17. Bicerano, J. *Prediction of Polymer Properties*; Marcel Dekker: New York, **1993**.
18. Razaifard, A. H.; Bader, M. G.; Smith, P. A. *Compos. Sci. Technol.* **1994**, *52*, 275.
19. Vanlandingham, M. R.; Eduljee, R. F.; Gillespie, J. W., Jr. *J. Appl. Polym. Sci.* **1999**, *71*, 699.